



Cite this: *RSC Appl. Polym.*, 2024, **2**, 32

# Thermoreversible gels for the encapsulation of macrophages: evaluation of polymer type on rheology and cytocompatibility

E. Zeqiri,<sup>a</sup> M. A. da Silva,<sup>id</sup> S. R. Aspinall,<sup>id</sup> E. Hoffman,<sup>b</sup> V. Hutter<sup>a,b</sup> and M. T. Cook<sup>id</sup>\*<sup>c</sup>

Thermoresponsive polymers have become a highly sought-after “smart material” due to their ability to modify their physical characteristics due to temperature changes. This research aimed to determine the biocompatibility of specific thermoreversible gels for immunocompetent cell models containing ImmuPHAGETM, human alveolar macrophage-like cells. Four polymers were selected based on their transition temperatures, including three commercially available pharmaceutical excipients, namely poloxamer 407, soluplus, and methylcellulose. The fourth system, poly(*N*-isopropyl acrylamide)-*b*-poly(ethylene oxide)-*b*-poly(*N*-isopropyl acrylamide), was synthesised in-house. Initially, the phase behaviour of these four polymers was evaluated visually by warming the polymer solutions and determining the state of the solution by vial inversion. Subsequently, a combination of rheological measurements was employed to compare the properties of these thermoreversible gels in culture media. The physical characterisation was followed by conducting cytocompatibility tests using human alveolar macrophages to assess their suitability as a scaffold for cell culture *in vitro* and to determine the cell response to different culturing environments. The study concluded that methylcellulose is the most promising and cost-effective material worth further exploration as a responsive matrix for immune cell encapsulation. Keywords: Thermoresponsive, Thermogelling, Alveolar macrophages, Foamy macrophages, immunocompetent *in vitro* models.

Received 22nd May 2023,  
Accepted 2nd November 2023

DOI: 10.1039/d3lp00056g

[rsc.li/rscapppolym](https://rsc.li/rscapppolym)

## Introduction

Alveolar macrophages are the most abundant antigen-presenting cells in the lungs, where they play a crucial role in regulating immune responses to inhaled substances and allergens.<sup>1</sup> It is well established that they are the first line of defense against inhaled substances in the lower airways.<sup>2</sup> However, while their roles in alveolar homeostasis, infection, and disease are relatively well understood, their role in inhaled toxicity is poorly defined.<sup>3</sup> Alveolar macrophages initiate and perpetuate local pulmonary responses, and observations from lung tissue slices from pre-clinical rodent studies have caused uncertainty and confusion for many pre-clinical safety assessments. One-third of candidate inhaled medicines fail in pre-clinical *in vivo* rodent studies due to the presence of abnormal alveolar macrophage morphology, whereby the cells take on a highly

vacuolated or foamy appearance.<sup>2,3</sup> Foamy alveolar macrophages (FAM) are enlarged lung macrophages with a highly granular or vacuolated cytoplasmic appearance when viewed under a light microscope and are due to an accumulation of lipids, drug particles, or other pathophysiological processes involved.<sup>3,4</sup> A foamy alveolar macrophage-FAM appearance may also be accompanied by an increased number of macrophages and monocytes that infiltrate the airways from the blood, which, according to Nikula *et al.*, may represent an adaptive response to administered particles or the initial stage of an adverse effect.<sup>4</sup> Therefore, alveolar macrophages are an attractive test system for assessing the cellular response to inhaled drugs. Creating *in vitro* 3D models that better mimic the natural extracellular matrix these immune cells would encounter *in vivo* may improve cellular functionality and provide improved responses for more representative and predictive macrophage cell responses to toxic stimuli. A more *in vivo*-like environment may be achieved using hydrogels in which the cells can be encapsulated as part of an immunocompetent cell model.

Hydrogels are three-dimensional cross-linked networks of hydrophilic polymers swollen in water.<sup>5</sup> These gels may be

<sup>a</sup>Centre for Topical Drug Delivery and Toxicology School of Life and Medical Sciences, University of Hertfordshire, Hatfield, Hertfordshire, AL10 9AB, UK

<sup>b</sup>ImmuONE Ltd, Science Building, College Lane, Hatfield, Herts AL10 9AB, UK

<sup>c</sup>UCL School of Pharmacy, University College London, London WC1E 6BT, UK

E-mail: [michael.t.cook@ucl.ac.uk](mailto:michael.t.cook@ucl.ac.uk)

supported by physical cross-links as an entangled network consolidated by non-covalent interactions or chemical cross-links consisting of covalent bonds between polymers. Physical cross-links may be reversed by external stimuli such as heat, changes in pH, or changes in salt content, whereas chemical cross-link hydrogels are typically only degraded by harsh external reagents that degrade covalent bonds.<sup>6</sup> The ability to switch cross-linking in response to external stimuli makes these physical hydrogels attractive “stimuli-responsive” materials for scientific research. In most cases, such conformational transitions are reversible, hence these hydrogels are capable of returning to their initial state as soon as the trigger is removed.<sup>7</sup> Stimuli-responsive hydrogels are seen as potential biomaterials or bio-inks where their controllable physical properties enable researchers to easily encapsulate and culture cells<sup>8</sup> within hydrogels for purposes such as the delivery of therapeutic cells to the body,<sup>9</sup> drug and gene delivery,<sup>10,11</sup> tissue engineering<sup>12</sup> and bioprinting.<sup>13</sup> Temperature-sensitive hydrogels can change their physicochemical properties in response to temperature, and “thermoreversible” hydrogels use temperature as external stimuli to induce sol-gel or gel-sol transition. Sol-gel materials are particularly attractive for maintaining a gel state when heated, which can be exploited for applications such as cell culture, where cells can be cultured in the gel state and isolated simply by cooling the system to room temperature. These materials could be mixed with cells and printed into multicomponent immunocompetent *in vitro* models containing immune cells, which are seen as a crucial milestone on the path to animal-free toxicological models. However, the compatibility of different thermoreversible hydrogels with immune cells is poorly understood. There is a need for studies on cellular compatibility of thermoreversible gels, particularly immune cells where both viability and functional end points need to be established to prove utility. In these systems, relationships between polymer chemistry, mechanisms of gelation, rheology and utility are unknown.

This study evaluates the suitability of thermoreversible gels for use in immunocompetent cell models containing alveolar macrophages. Polymers were chosen based on their range of LCST to allow switching between liquid and gel states when heated from room to culture temperatures (around 37 °C), based on prior studies. Furthermore, commercially-available systems with a history of use in pharmaceuticals were included, along with a synthetic poly(*N*-isopropyl acrylamide)-*b*-poly(ethylene oxide)-*b*-poly(*N*-isopropyl acrylamide) (PNIPAM-*b*-PEO-*b*-PNIPAM) material to probe the utility of synthetic block copolymer architectures in this application using an architecture and molecular weight known to give thermoreversible gelation.<sup>14</sup> The rheology of Poloxamer 407, Soluplus, Methylcellulose (MC), and PNIPAM-*b*-PEO-*b*-PNIPAM (Fig. 1) were studied to compare their properties as thermoreversible gels. Following this, the compatibility of alveolar macrophage-like cells with the materials was assessed using membrane integrity and mitochondrial activity endpoints. The study's outcomes will inform the selection of thermoreversible gels for generating immunocompetent models in future work, as well as guide material development for outside applications such as tissue engineering, regenerative medicine, and therapeutic cell delivery.

Poloxamer 407 is a water-soluble non-ionic ABA triblock copolymers consisting of central hydrophobic blocks of polypropylene glycol (PPO) flanked by two hydrophilic blocks of polyethylene glycol (PEO) with the degree of polymerisation PEO<sub>100</sub>-PPO<sub>65</sub>-PEO<sub>100</sub>.<sup>15,16</sup> The thermoreversible gelling property of these polymers results from their temperature-dependent ability to self-assemble into micelles in solutions and then form a liquid crystalline gel when the fraction of micelles in solution is greater than ( $\phi > 0.53$ ).<sup>17</sup> Poloxamer 407 is soluble in cold water, but as temperature increases, copolymer molecules aggregate into micelles due to the dehydration of hydrophobic propylene oxide blocks to form a spherical micelle core with an outer shell of hydrated swollen polyethyl-

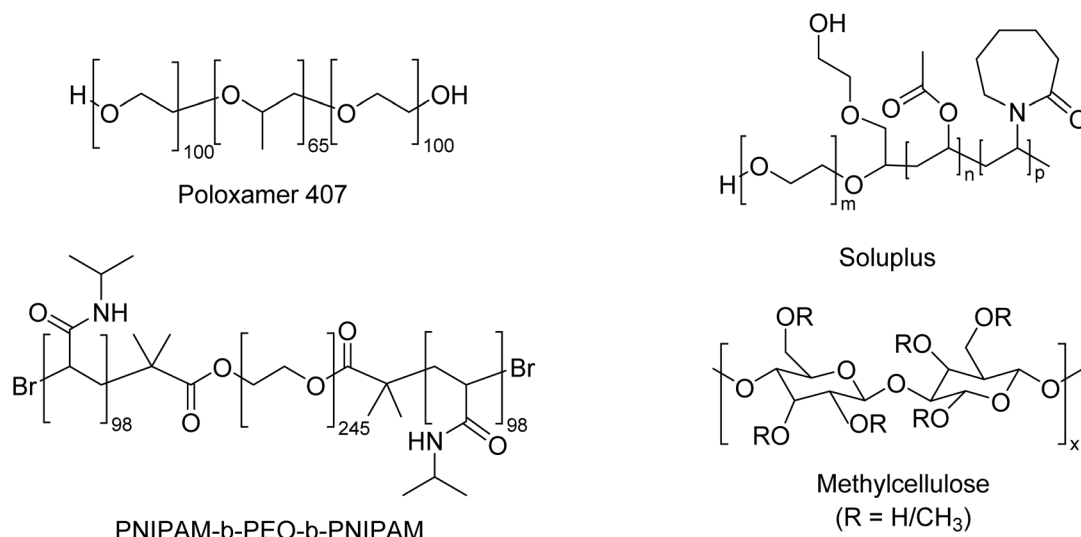


Fig. 1 Chemical structures of the thermoreversible gelators used in this study.



ene oxide.<sup>18</sup> When the phase volume of micelles is greater than 0.53, the gel phase is obtained. The transition of PPO from a relatively hydrophilic to a relatively hydrophobic state when heated above a critical temperature can be seen as an example of a lower critical solution temperature (LCST), commonly used as a trigger in sol-gel systems. Poloxamer 407 is an attractive thermoreversible gel as it shows low viscosity at room temperature, enabling easy manipulation such as pipetting or injecting gels at physiological temperatures (~37 °C). Furthermore, it is currently used as a pharmaceutical excipient, mitigating toxicological risks.<sup>16</sup>

Soluplus (*N*-vinyl caprolactam)-poly(vinyl acetate)-poly(ethylene glycol) is a poly graft copolymer with a molecular weight of 90–140 kg mol<sup>-1</sup>, manufactured by BASF.<sup>19</sup> It is an amphipathic copolymer that can form micelles when its concentration exceeds its CMC.<sup>20</sup> Aqueous solutions of Soluplus increase in viscosity upon warming, dependent upon concentration and co-solutes.<sup>19</sup> The amphipathic nature of Soluplus leads to the formation of spherical “fuzzy” micelles in cool aqueous solutions.<sup>21</sup> Upon heating, the LCST behaviour of poly(*N*-vinylcaprolactam) can drive that component from hydrophilic to a more hydrophobic state.<sup>22</sup> In other poly(*N*-vinylcaprolactam) systems, this promotes physical interaction between polymers and the formation of a gel state.<sup>22,23</sup> Whilst the process has not been studied in detail, this trigger likely drives the temperature-dependent rheological changes observed in Soluplus.<sup>19,24</sup>

Methylcellulose is a hydrophobically-modified cellulose with a typical degree of methyl substitution between 1.4 and 2.0 methoxy groups per glucose unit.<sup>25</sup> It shows a singular thermal behaviour in which aqueous solution viscosity remains constant or slightly decreases when its temperature increases up to a critical temperature point (29 ± 2 °C). If the temperature continues to increase, viscosity strongly increases, forming a thermoreversible gel.<sup>26</sup> In an aqueous solution of MC, there exist three possible intermolecular forces among MC chains or between MC and water: (1) hydrogen bonding between unmodified hydroxyl groups on MC chains, (2) hydrogen bonding between the hydroxyl groups of MC and water molecules, and (3) hydrophobic association between hydrophobic groups (*i.e.* methyl groups) on MC chains.<sup>27</sup> According to Kundu *et al.*, hydrogen bonding between MC chains and water is dominant at low temperatures to ensure the water solubility of MC. When the hydrogen bonding is broken upon heating, the so-called hydrophobic association becomes possible, followed by physical cross-linking and gelation.<sup>28</sup> These characteristics classify MC as an LCST-exhibiting polymer. To create gels with the desired thermoresponsive properties needed for this study, lower molecular weight MC was chosen as higher molecular weight MC leads to prohibitively viscous solutions at room temperature.<sup>25,29,30</sup>

Poly(*N*-isopropyl acrylamide) (PNIPAM) is one of the most studied synthetic thermosensitive polymers. Its extensive investigation is due to its LCST being close to body temperature, making it an attractive polymer for biomedical applications.<sup>31</sup> The LCST of PNIPAM is approximately 32 °C, which

may be altered through copolymerisation with hydrophilic monomer, changes in concentration, ionic strength and pH, but has a low dependence on molecular weight.<sup>23</sup> Whilst the homopolymer of PNIPAM typically forms a precipitate at elevated temperatures, including PNIPAM in copolymer architectures can permit gel formation instead. PNIPAM-*b*-poly(ethylene oxide) (PEO)-*b*-PNIPAM ABA copolymers exhibit thermoreversible gelation dependent upon the molecular weight of the blocks.<sup>14,20,32</sup> When each block has a molecular weight *ca.* 10 kDa, the polymer can form thermoreversible gels in which the gel state is maintained by spherical flower-like core-shell micelles with relatively hydrophobic PNIPAM in the core and PEO at the corona.<sup>32</sup> Elastically active unimer chains may then bridge adjacent micelles. PNIPAM has been used in research in tissue engineering to coat substrates upon which cells may be grown and attach above LCST (*ca.* 32 °C) but be detached with cooling below LCST.<sup>33</sup> However, PNIPAM-based material have not been incorporated in any approved medicine to date.<sup>23</sup>

This study reports the evaluation of four thermoreversible gels for the encapsulation of alveolar macrophages with a view to incorporating these materials in immunocompetent models through processes including 3D printing. The phase behaviour of the polymers is assessed in the presence of relevant culture media, and the cytocompatibility is assessed against human alveolar macrophages.

## Materials and methods

### Materials

Soluplus and Poloxamer 407 were procured from BASF (Ludwigshafen, DE). PNIPAM-*b*-PEO-*b*-PNIPAM was synthesised and characterised as reported previously.<sup>32</sup> The degree of polymerisation of the PNIPAM blocks was *ca.* 98, and the PEO segment was 245, with corresponding *M<sub>n</sub>* *ca.* 10–10–10 kDa. MC A15, propidium iodide, and Trypan blue were all purchased from Sigma-Aldrich (Poole, Dorset, UK). Water used in all formulations was deionised and sourced from a Millipore (Watford, Herts, UK) system. The CytoTox-ONE™ Homogeneous Membrane Integrity (LDH) and CellTiter 96® Aqueous One Solution Cell Proliferation Assay (MTS) kits were purchased from Promega (Southampton, Hampshire, UK). ImmuPHAGE™ (human alveolar macrophage-like cells) and ImmuPHAGE growth medium (complete culture medium, CCM) were provided by ImmuONE (Hatfield, Herts, UK). Cells were authenticated prior to experimentation and validated for macrophage and epithelial biochemical and physical characteristics, cell surface markers and functionality (ImmuONE, Hatfield, Herts, UK).

### Manufacture of hydrogels and characterisation

10 mL solutions of Poloxamer 407 and Soluplus were prepared in cell CCM in the range of 15–20% w/v. The powder was added slowly and stirred using a magnetic plate at 900 rpm in an ice bath. Once the polymers were entirely dissolved at *ca.* 1 °C, they were stored in the fridge at 4 °C overnight. Before



cell experiments, solutions were sterilised by filtering using a 0.22  $\mu\text{m}$  filter. MC solutions were formed by the dispersion technique, where approximately half of the required volume of completed cell medium was warmed to 40  $^{\circ}\text{C}$ , then added into MC powder and stirred in until thoroughly dissolved. The remainder of the solvent was then added and stirred until the entire polymer was dissolved. The solutions were then allowed to equilibrate overnight in a 4  $^{\circ}\text{C}$  refrigerator. The MC solutions were sterilised by autoclaving the solution at 120  $^{\circ}\text{C}$  for 20 min. Different sterilisation methods for MC solutions has previously been explored which found that autoclaving, considered the most effective way for sterilising all biological life, did not modify MC structure.<sup>34</sup> The thermoreversible gelation phenomena of solutions were visually observed by testing their sol-gel temperature transformation during heating in a water bath. The sol-gel transformation features were ranked as: “liquid” (flows freely upon inversion), “viscous” (flows slowly upon inversion) and “gel” (the solution did not flow upon inversion).

Rheological analysis of polymer solutions was conducted on a TA instruments AR1500EX rheometer with a Julabo AWC100 cooling unit (UK) equipped with a 40 mm parallel plate geometry. Experiments were run with a 2 min equilibration time at the required temperature and a gap of 1 mm. Strain sweeps were initially conducted at an angular frequency of 6.283 rad per s at 37  $^{\circ}\text{C}$ . This allowed the identification of a strain within the linear viscoelastic region, defined as the region at low shear where the storage ( $G'$ ) and loss ( $G''$ ) moduli are independent of strain, for further rheological analysis. Frequency sweeps were conducted at 1% strain (within the linear viscoelastic region) at 37  $^{\circ}\text{C}$ , between 0.628 and 628 rad per s angular frequency. Temperature ramps were then conducted at 6.283 rad per s angular frequency and a strain of 1%, ramping between 20 and 40  $^{\circ}\text{C}$  for PNIPAM-*b*-PEO-*b*-PNIPAM, poloxamer 407 and soluplus solutions, and between 20 and 55  $^{\circ}\text{C}$  for MC solutions, at a rate of 1  $^{\circ}\text{C min}^{-1}$ . Flow rheology was conducted at 25  $^{\circ}\text{C}$  to characterise the behaviour of the solutions during manipulation at room temperature. In these experiments, shear rate was varied between 3 and 40  $\text{s}^{-1}$ . Where required, gelation time was determined by holding temperature at 37  $^{\circ}\text{C}$  without equilibration prior and conducting measurements at 1% strain and an angular frequency of 6.283 rad per s with time.

### Cell encapsulation

To investigate whether Poloxamer407, Soluplus, MC and PNIPAM support the growth of ImmuPHAGE<sup>TM</sup>, these cells were incorporated into a hydrogel matrix and incubated for 24 h–48 h, after which cell viability and cytotoxicity assays were performed.

Cells were harvested by gently scraping them from T75 flask, and their viability was assessed by the trypan blue cell exclusion assay and cells counted manually using a haemocytometer. For experiments, cells (400 cells per  $\mu\text{L}$ ) were transferred into the hydrogel (500  $\mu\text{L}$  in 24 well plate, 100  $\mu\text{L}$  in 96 well plate), followed by gentle manual mixing to ensure hom-

ogenous distribution of cell suspension in the polymer. Cells were seeded in a density of  $4 \times 10^4$  cells per well in 100  $\mu\text{L}$  in 96 well plate for Poloxamer 407, Soluplus and PNIPAM-*b*-PEO-*b*-PNIPAM. However, MC solutions seeded at a density of  $2 \times 10^5$  cells per well in 500  $\mu\text{L}$  in 24 well plate due to the increased viscosity of the gel.

### Mitochondrial activity and cytotoxicity assessment

The CellTiter 96®Aqueous One Solution Cell Proliferation Assay (MTS) reagent was used for the quantification of viable cells according to the manufacturer's instructions. A 20  $\mu\text{L}$  aliquot of MTS reagent was added to each well containing 100  $\mu\text{L}$  cell suspension and incubated for 4 h at 37  $^{\circ}\text{C}$ , 5% v/v  $\text{CO}_2$  in a humidified incubator. The formation of formazan was quantified by measuring the absorbance at 492 nm using an absorbance plate reader (CLARIOstar, BMG LABTECH, DE).

In the present study, a range of gel systems with different properties was used, which resulted in many experimental challenges. Some gels were incompatible with certain assays used, however, the principle of the assay, endpoint measured, and data analysis was kept the same. Membrane permeability was identified as a key indicator of cell death<sup>35</sup> and was used as an additional endpoint for cell viability in this study. While the MTS assay was compatible with all tested polymers, there were three methods for membrane permeability utilised depending on various physical properties of tested hydrogels: (i) the CytoTox-ONE<sup>TM</sup> Homogeneous Membrane Integrity Assay for PNIPAM, (ii) Trypan blue exclusion assay for Poloxamer 407 and Soluplus and (iii) propidium iodide exclusion assay for MC.

The CytoTox-ONE<sup>TM</sup> Homogeneous Membrane Integrity Assay was used to determine extracellular lactate dehydrogenase (LDH) concentration. In brief, 50  $\mu\text{L}$  of cell supernatant was incubated with 50  $\mu\text{L}$  CytoTox-ONE<sup>TM</sup> reagent in the dark for 10 min at 22  $^{\circ}\text{C}$ , followed by the addition of 25  $\mu\text{L}$  stop solution. Triton X-100 was used as a control (0.1% v/v in CCM). Fluorescence was measured at 560 excitation wavelength and 590 nm emission wavelength. Cell death was calculated as a percentage of dead cells compared to positive control. Poloxamer 407 and Soluplus were autofluorescent, while MC was too viscous to get manipulated in small volumes therefore, the membrane integrity assessment for Poloxamer 407 and Soluplus was performed with trypan blue (which was not compatible with MC due to staining of the polymer) and MC with propidium iodide.

Cell count and cell viability were assessed using the trypan blue exclusion assay. Trypan blue 0.4% w/v dye was added to an equal volume of cell suspension (50  $\mu\text{L}$ ), mixed using a vortex mixer and 10  $\mu\text{L}$  transferred onto a haemocytometer. All cells (stained and non-stained with trypan blue) were counted in four 1 mm squares, which indicates a 0.1  $\text{mm}^3$  volume. Cell concentration per mL was calculated as the average number of total cells in four squares multiplied by the dilution factor (2) and multiplication factor for 1 mL volume ( $\times 10^4$ ). Cell death was calculated as a percentage of stained cells in the total cell count.





Cytotoxicity assessment with PI were performed using PI solution  $2 \mu\text{g mL}^{-1}$ .  $2 \mu\text{L}$  of PI was added to  $200 \mu\text{L}$  cell suspension and incubated at room temperature for 10 min.  $10 \mu\text{L}$  of PI-cell suspension mixture was transferred onto a haemocytometer and viewed using a fluorescent microscope ex 535 nm:em 617 nm (Invitrogen™ EVOS™ ThermoFisher). Cell concentration was calculated as the average number of total cells in four squares times with a multiplication factor for 1 ml volume ( $\times 10^4$ ). Cell death was calculated as a percentage of stained cells with PI in the total cell count.

### Cell functionality assessment

In accordance with the literature, alveolar macrophages display phagocytic activity.<sup>36</sup> Therefore, to determine the impact of MC on the phagocytic ability of ImmUPHAGE, cells were incubated for two hours in the dark with uniform  $1.0 \mu\text{m}$  carboxylate-modified microspheres at a ratio of 1:30 (cells: particles). Each sample was diluted with  $150\text{--}200 \mu\text{L}$  CCM before centrifugation (7 rpm/5 min). Cells were washed twice with PBS before fixation with 3.7% w/v paraformaldehyde for 15 min. Following this, PFA was removed, and samples were resuspended in  $900 \mu\text{L}$  of PBS for flow cytometry. Five thousand events per sample were counted, and cells were identified from particles and cellular debris by their forward and side scatter. The engulfed fluorescent beads were measured by flow cytometry Guava EasyCyte system (Guava EasyCyte 8HT, Millipore, UK) ex 505 nm:em 515 nm.

### Statistical analysis

Statistical analysis was conducted using GraphPad Prism (Version 9.2.0) software (USA). Data were analysed by one-way ANOVA with *post-hoc* Bonferroni test or Student's *t*-test where appropriate. Data are presented as means  $\pm$  standard deviation.

## Results

### Evaluation of thermoreversible hydrogels

The phase behaviour of each thermoreversible hydrogel was initially evaluated macroscopically by warming solutions of the polymer dissolved in CCM. The increase in viscosity was deter-

mined by a vial inversion as a typical screening tool to identify potential gelation, but confirmation was compiled by rheology. This approach intended to identify solutions which transitioned to a gel state between room (*ca.*  $20^\circ\text{C}$ ) and culture ( $37^\circ\text{C}$ ) temperature to allow manipulation at room temperature but gelation upon placement in an incubator. As such, concentrations were identified with the criterion: sol-gel transition ( $T_{\text{gel}}$ ) occurring at  $20^\circ\text{C} < T_{\text{gel}} < 37^\circ\text{C}$ . For poloxamer 407, this was the concentration range 18–20% w/v (Table 1). Soluplus exhibited the required  $T_{\text{gel}}$  at 18–20% w/v, PNIPAM-*b*-PEO-*b*-PNIPAM required 20% w/v, whilst MC required only 6–8% w/v, however it was noticeably more viscous at room temperature due to the ease at which it swells at low concentrations and its polymer-polymer interactions. This pilot study helped to identify concentrations for a thorough rheological analysis.

The polymers selected show distinct pathways to gel formation, which in part explain the different phase behaviours. Poloxamer 407 switches from liquid to gel as the result of a temperature-driven shift to an abundance of spherical micelles with PPO core and PEO shell which pack into a face-centered cubic phase. Thus, gel phase exist only in the condition that there is sufficient volume fraction of micelles to allow packing into this mesophase, giving the concentration-dependence observed. Soluplus gelation mechanism is poorly understood. However it is known that concentrated soluplus solutions contain “fuzzy” micellar structures which pack into a concentrated phase following Teubner–Strey models.<sup>21</sup> Thus, gelation is favoured, occurring at lower temperatures, in more concentrated systems. Thermoresponsive behaviour in this system is imparted by the poly(*N*-vinylcaprolactam) component which exhibits an LCST and is presumed to lead to greater hydrophobicity of the system above LCST, favouring soluplus–soluplus inter-micellar interactions. PNIPAM-*b*-PEO-*b*-PNIPAM also achieved gel formation *via* supracolloidal structures, with the LCST transition of PNIPAM leading to the formation of “flower-like” micellar structures with PNIPAM core and PEO shell which can be bridged by unimer chains, favouring gelation when the phase volume of the micelle is sufficient to allow a network to be formed.<sup>32</sup> Poloxamer, Soluplus, and PNIPAM-*b*-PEO-*b*-PNIPAM contain LCST-exhibiting blocks, and it is known that at high concentrations the solvation of these

**Table 1** The physical state of poloxamer 407, Soluplus, MC, and PNIPAM-*b*-PEO-*b*-PNIPAM in cell culture medium with variations of concentration and temperature. L (blue) is a liquid, V (pink) is a viscous liquid, and G (green) is a gel

Conc. (% w/v) Temp. °C	Poloxamer 407				Soluplus				MC				PNIPAM- <i>b</i> -PEO- <i>b</i> -PNIPAM		
	15%	16%	18%	20%	15%	16%	18%	20%	5%	6%	7%	8%	10%	15%	20%
6	L	L	L	L	L	L	L	L	V	V	V	V	L	L	L
10	L	L	L	L	L	L	L	L	V	V	V	V	L	L	L
15	L	L	L	V	L	L	V	V	V	V	V	V	L	L	L
21	L	V	V	G	L	L	V	V	V	V	V	V	L	L	L
25	V	V	G	G	L	L	V	V	V	V	V	V	L	L	V
30	V	V	G	G	L	L	V	V	V	V	V	V	L	L	V
35	V	G	G	G	V	V	G	G	V	G	G	G	L	L	G
37	V	G	G	G	G	G	G	G	G	G	G	G	L	V	G



moieties can be reduced, favoring phase separation at lower temperatures.<sup>23</sup> MC exhibits thermogelation *via* hydrophobic effects on the methoxy-substituted hydroxyl groups to give physically-entangled polymer networks.<sup>37</sup> The much lower concentration of MC required is likely a driving factor in the relatively flat transition temperature measurements with concentration.

Rheological profiling of the polymer solutions in growth medium was conducted by small-amplitude shear rheometry with varying temperatures to determine  $T_{\text{gel}}$ , defined as the temperature at which the material transitioned from predominantly viscous ( $G'' > G'$ ) to predominantly elastic ( $G' > G''$ ) (at 6.283 rad per s, 0.1% strain).<sup>38</sup> This criterion may be simplified by the use of the loss tangent, the tangent of the phase angle ( $\delta$ ) between stress and strain, which has an identical value to  $G''/G'$ . As such,  $T_{\text{gel}}$  may be defined as a transition from  $\tan \delta > 1$  to  $\tan \delta \leq 1$ . Furthermore, oscillatory frequency and amplitude sweeps were conducted on the gel state at 37 °C to characterise the gels. In brief, amplitude sweeps showing the relationship between  $G'$  and  $G''$  on strain may determine a first Newtonian plateau (the linear viscoelastic region), which terminates at a yield strain, above which the internal structure of the material is altered by the strain imposed upon it. A frequency sweep conducted at a strain below the yield (in this case, 0.1% strain) allows the viscoelastic spectrum to be explored, which is characteristic of specific categories of material. Gels are typically considered to exhibit a low dependence of  $G'$  and  $G''$  on angular frequency with  $G' > G''$ , and the magnitude of these values indicates the resistance to shear. Small amplitude oscillatory frequency sweeps and amplitude sweeps have previously been conducted on lung tissue, giving approximated values of 0.9 and 0.3 kPa for  $G'$  and  $G''$  (at 1 Hz), respectively, with a yield stress of *ca.* 1%.<sup>39</sup> Finally, flow rheology was conducted at room temperature (20 °C) to evaluate the ability to manipulate the materials at room temperature, for example, by pipetting or printing. These flow curves relate shear rate to apparent viscosity of the material (resistance to deformation), allowing determination of how “thick” the material is and whether this is dependent upon the shear that is imposed upon it.

Poloxamer solutions at 16 and 18% w/v exhibited a clear sol–gel transition by rheometry (Fig. 2a). At 20 °C the polymer solution had low values of  $G'$  and  $G''$ , which abruptly increased in absolute value at *ca.* 24 and 27 °C, for 16 and 18% w/v solutions, respectively, with concurrent gelation ( $\tan \delta < 1$ ). Above  $T_{\text{gel}}$ , the material plateaued at *ca.* 9 and 16 kPa. Increasing the concentration to 20% w/v did not substantially increase the strength of the material ( $G'$  *ca.* 17 kPa), but due to more polymer interactions such as entanglement, the solutions were viscous even at 20 °C. Flow rheograms at 20 °C indicated that the materials were highly shear thinning, potentially aiding pipetting and spreading, but in the case of the 20% w/v solutions, had very high initial viscosity (Fig. 2b). Frequency sweeps at 37 °C indicated a gel-like low dependence of  $G'$  and  $G''$  on frequency, with  $\tan \delta < 1$  at all concentrations (Fig. 2c), indicative of the formation of the packed micellar phase. Amplitude sweeps demonstrated poloxamer's brittle character, sharply

yielding at 0.4 and 1.2% at 16 and 18%, respectively (Fig. 2d) as the face-centred cubic mesophase is disrupted at low strains.

Soluplus solutions were studied with the same rheological tests as poloxamer. Temperature ramps (Fig. 3a) demonstrated clear increases in viscosity with temperature, with a sharp rise at *ca.* 30–35 °C leading to a material with  $G'$  reaching a maximum of *ca.* 100 Pa, but with  $\tan \delta \approx 1$ . Flow rheology (Fig. 3b) showed that the Soluplus solutions had very low viscosity at 20 °C, with shear-thinning behaviour, regardless of concentration. Thus, Soluplus solutions were exceedingly easy to manipulate at room temperature. Different behaviour was observed when investigating the more viscous state at 37 °C. Frequency sweeps showed that the materials behaved as viscoelastic liquids meeting the condition  $G' > G''$  at 1.254 rad per s (for 18 and 20% w/v concentrations), giving a characteristic relaxation time of 0.8 s at all concentrations, indicating shear-induced entanglements in the system. At longer timescales the material relaxes and flows. Strain sweeps demonstrated that the materials did not exhibit sharp yields, instead exhibiting a broad flow point at *ca.* 30% strain, consistent with a lack of well-defined gel structure.

MC solutions exhibited thermogelation in CCM, as determined by rheometry. Temperature scans (Fig. 4a) indicated that  $T_{\text{gel}}$  appeared at elevated temperature compared to the vial inversion tests (Table 1), giving values of 45 and 43 °C for 7 and 8 wt%. The discrepancy was postulated to be a kinetic effect and that the gelation processes may be slow thus, the samples were held at a low frequency (1 Hz) and strain (0.1%) at 37 °C and the evolution of rheological response determined with time (Fig. 4b). 7 and 8 wt% MC solutions took 34 and 12 min to reach a gel state under this regime, respectively. Evaluation of the gel state by frequency sweep at 37 °C (Fig. 4c) demonstrated that the materials were a gel in this state, with  $\tan \delta < 1$  across the range measured. The storage moduli of the materials were between *ca.* 400 and 700 Pa in this range, with the 8% w/v material having a larger elastic modulus. Amplitude sweeps showed yields at 20 and 5% strain for 7 and 8% w/v MC, respectively, indicating an increasingly brittle character in the more concentrated system (Fig. 4d). Flow rheology indicated that the materials had limited pseudoplastic behaviour, in-line with the experimental observation that the solutions were challenging to pipette (Fig. 4e), indicating that minimal reordering of the polymers occurs when increased shear rate is applied.

PNIPAM-*b*-PEO-*b*-PNIPAM solution in CCM were studied with the same rheological tests as previous polymers. Temperature ramps indicate that PNIPAM-*b*-PEO-*b*-PNIPAM solution at 20% exhibited transition with increased temperature, with a steep rise occurring at *ca.* 30 °C (Fig. 5a), reaching a maximum of 100 Pa at 40 °C. Flow rheology showed that at 20 °C, the PNIPAM-*b*-PEO-*b*-PNIPAM solution was highly shear thinning, showing Newtonian behaviour at higher range of share rate (Fig. 5). Frequency sweep tests at 37 and 55 °C (during and above transition) showed that the material behaved as a viscoelastic liquid with Maxwell-type behaviour, with the relaxation time increased at higher temperatures



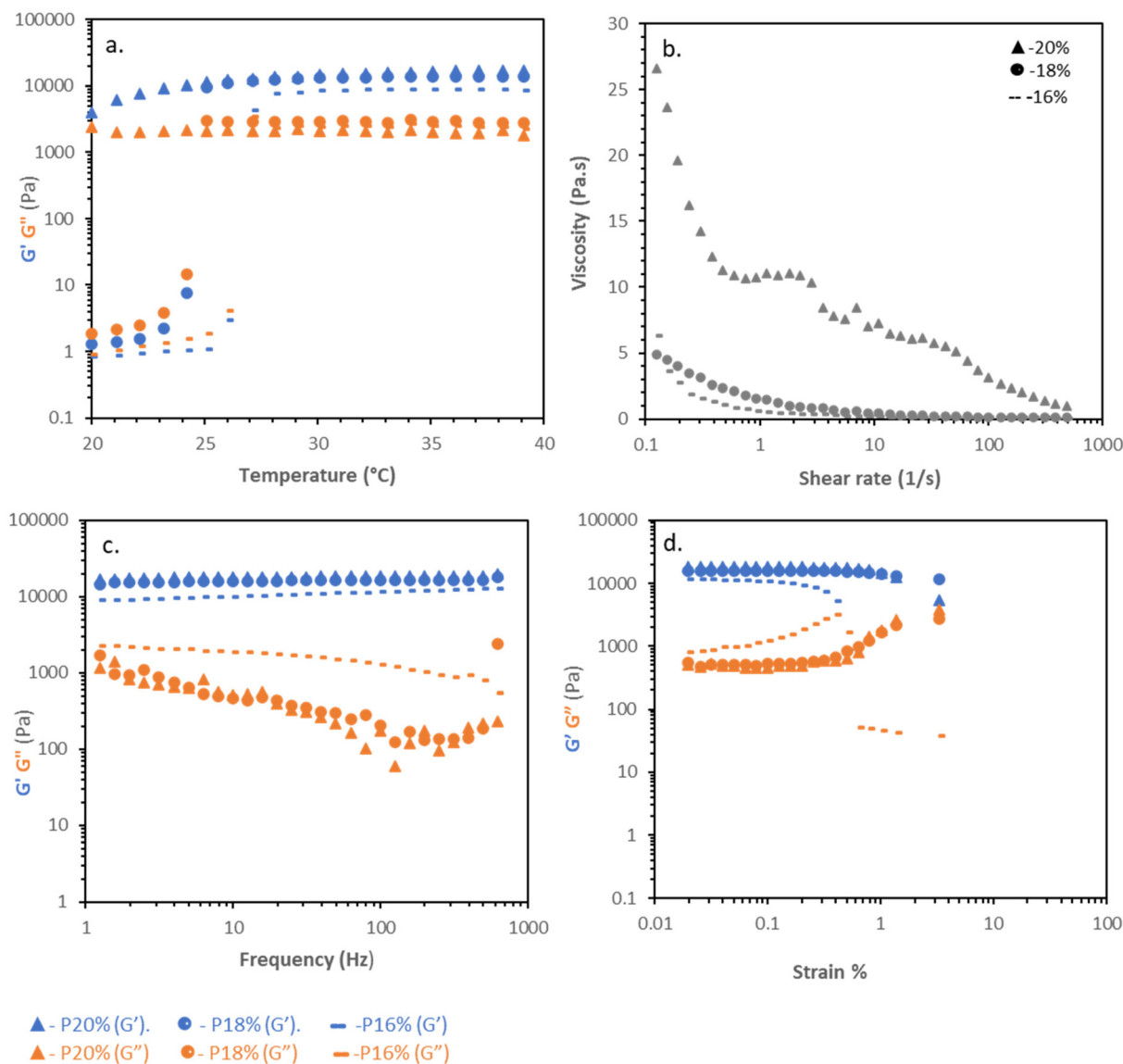


**Fig. 2** Rheological properties of Poloxamer407(P) solutions at concentrations 16%, 18% and 20% (w/v) in CCM: (a) temperature ramps at a fixed strain (0.1%) and frequency (6.283 rad per s). (b) Flow rheology at 20 °C. (c) frequency sweeps at 0.1% strain and 37 °C. (d) Amplitude sweeps at 6.283 rad per s and 37 °C.

(Fig. 5c). This indicates that the micellar network in the system is transiently induced by shear, assumed to be related to forced interaction of the polymer colloids, the persistence of which increases at higher temperatures where the PNIPAM blocks are desolvated to a greater extent. Amplitude sweeps further demonstrated the viscous-liquid type behaviour at 37 °C, with no apparent yield observed, until further heating at 55 °C (Fig. 5d) where the amplitude sweeps are measured at a higher frequency than the  $G'/G''$  cross-over (Fig. 5c and e).

#### Evaluation of compatibility of thermoreversible hydrogels with immune cells

The biocompatibility of each hydrogel was evaluated by assessment of mitochondrial activity and cytotoxicity of immune cells (ImmuPHAGE) encapsulated in gels. Cells were incorpor-

ated into a hydrogel matrix and incubated for up to 48 h. Cells showing high viability within hydrogels were further evaluated to assess their functionality. The mitochondrial activity of cells embedded into Poloxamer 407 (Fig. 6a) and Soluplus (Fig. 6c) were significantly ( $p < 0.001$ ) reduced to ~7% in comparison with cells maintained in CCM. Additionally, the concentration of extracellular LDH was significantly ( $p < 0.001$ ) increased after 24 h exposure to appointed hydrogels, indicating a compromised cell membrane in cells embedded in these polymers (Fig. 6b and d). This suggests that the health of cells was highly affected by Poloxamer 407 and Soluplus, with the majority of cells (>90% cell death) occurring after 24 h exposure.

Cells embedded in MC hydrogels showed significantly ( $p < 0.001$ ) reduced metabolic activity after 24 h incubation, which was followed by cell recovery after 48 h when there was



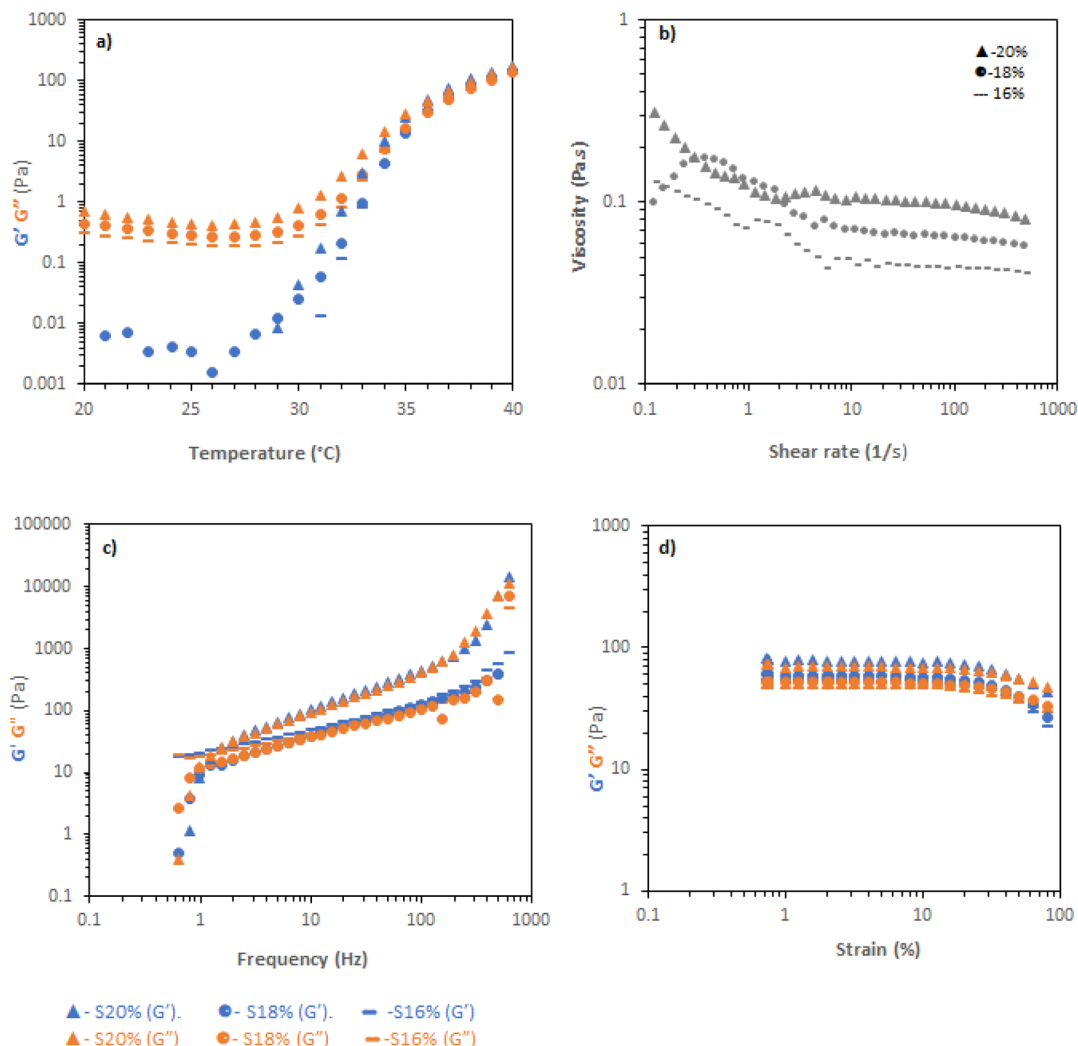


**Fig. 3** Rheological properties of Soluplus(S) solutions at concentrations 18% and 20% (w/v): (a) temperature ramps at a fixed strain (0.1%) and frequency (6.283 rad per s). (b) Flow rheology at 20 °C. (c) frequency sweeps at 0.1% strain and 37 °C. (d) Amplitude sweeps at 6.283 rad per s and 37 °C.

no significant difference in metabolic activity of cells seeded in gel and those in CCM (Fig. 7a). This might be an adaptive response due to cells being exposed to different environments. Cells seeded in MC 8% (MC 8%) showed an increase in membrane permeability after 24 h, followed by cell recovery after 48 h (Fig. 7b). Additionally, phagocytic activity as a core function of immune cell functionality was examined (Fig. 7c). After 24 h and 48 h incubation, 92% and 86% of the cells incorporated into the MC matrix showed phagocytic properties, respectively. There was no significant difference ( $p > 0.05$ ) in phagocytic activity of cells in the hydrogel in comparison with the control cells in CCM.

The compatibility of PNIPAM solutions with ImmuPHAGE cells were assessed using metabolic activity (Fig. 8a) and membrane integrity (Fig. 8b) to indicated viability and phagocytic activity (c) to support functionality assessment. Whilst PNIPAM caused a significant reduction ( $p < 0.001$ ) in mitochondria activity (decreased to 50% compared to control), the

extracellular concentration of LDH expressed as percentage of dead cells showed no significant difference ( $p > 0.05$ ). The phagocytic activity of ImmuPHAGE in PNIPAM was significantly reduced ( $p < 0.001$ ) after 24 h to 65%, but after 48 h, cells showed similar phagocytic response as those in CCM.

## Discussion

Gels from animal origins have been widely used as substrates for 3D cell culture, where the best known is Matrigel – extracted from mouse sarcoma, a tumour rich in ECM proteins.<sup>40</sup> However, animal gel systems may contain biological proteins, growth factors or xenogeneic components, which can lead to activation of immune cells. There are also cost and composition variability issues that may show batch-to-batch variation that could lead to inconsistent results and reflect in the experimental endpoints.<sup>40,41</sup> Therefore, gels produced





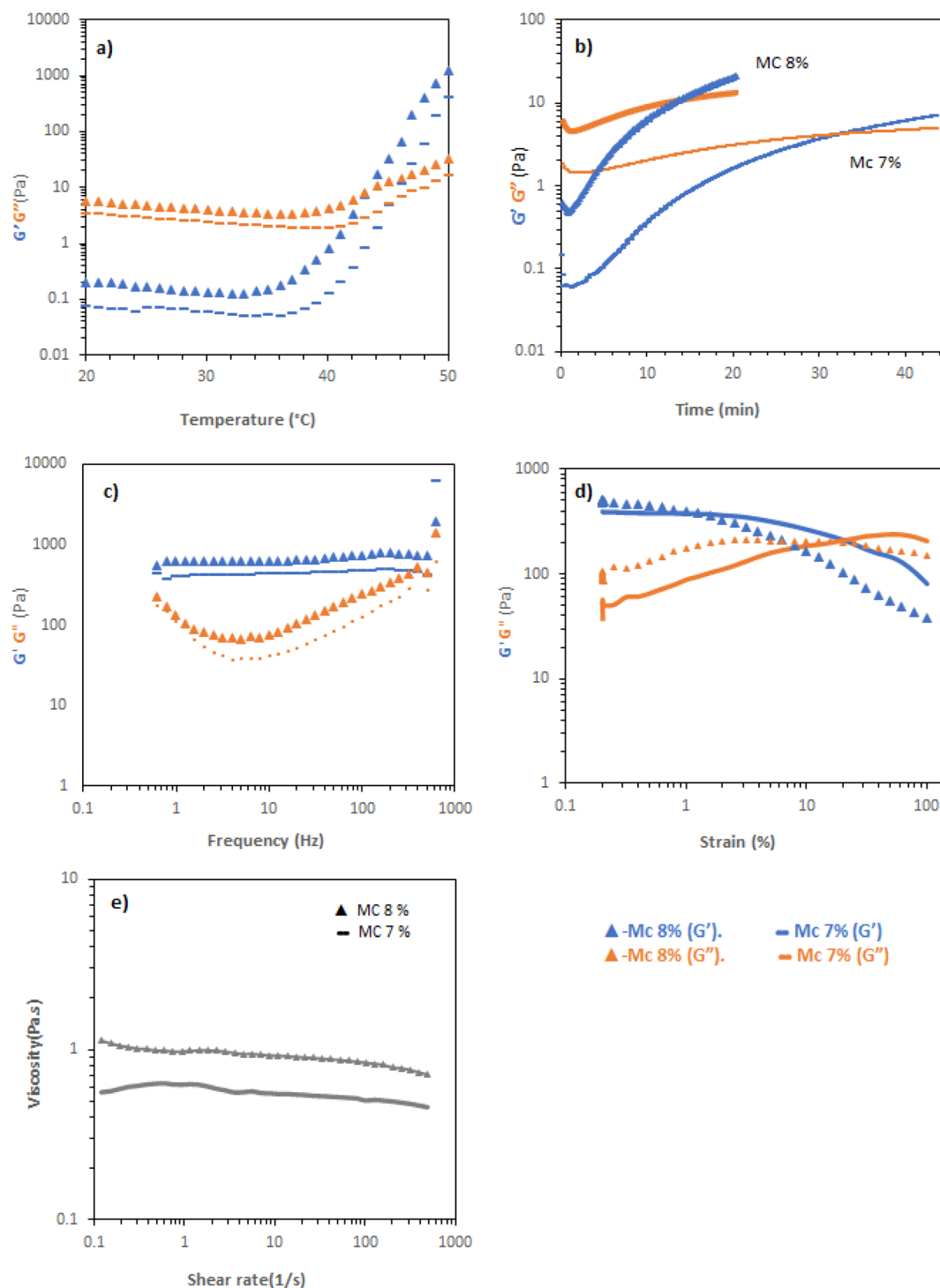


**Fig. 4** Rheological properties of MC at concentration 7% and 8% w/v (MC 7% and MC 8%, respectively): (a) temperature ramps at a fixed strain (0.1%) and frequency (6.283 rad per s). (b) Time-dependence of rheological response (0.1% strain, 6.283 rad per s) at 37  $^{\circ}\text{C}$ . (c) Frequency sweeps at 0.1% strain and 37  $^{\circ}\text{C}$ . (d) Amplitude sweeps at 6.283 rad per s and 37  $^{\circ}\text{C}$ . (e) Flow rheology at 20  $^{\circ}\text{C}$ .

from defined polymeric composition with natural or synthetic composition are attractive biomaterials for cell culture *in vitro*.<sup>8</sup> Since culturing conditions have a fundamental role in the survival, proliferation, and differentiation of the cells, it is crucial to pay attention to the physical properties of their

environments. For example, Bystroňová *et al.* demonstrated the impact of stiffness on monocyte growth and proliferation, so cells cultured in soft hydrogels mimicked suspension-like growth and had high metabolic activity.<sup>42</sup> Additionally, several studies have shown that macrophages phenotype can be



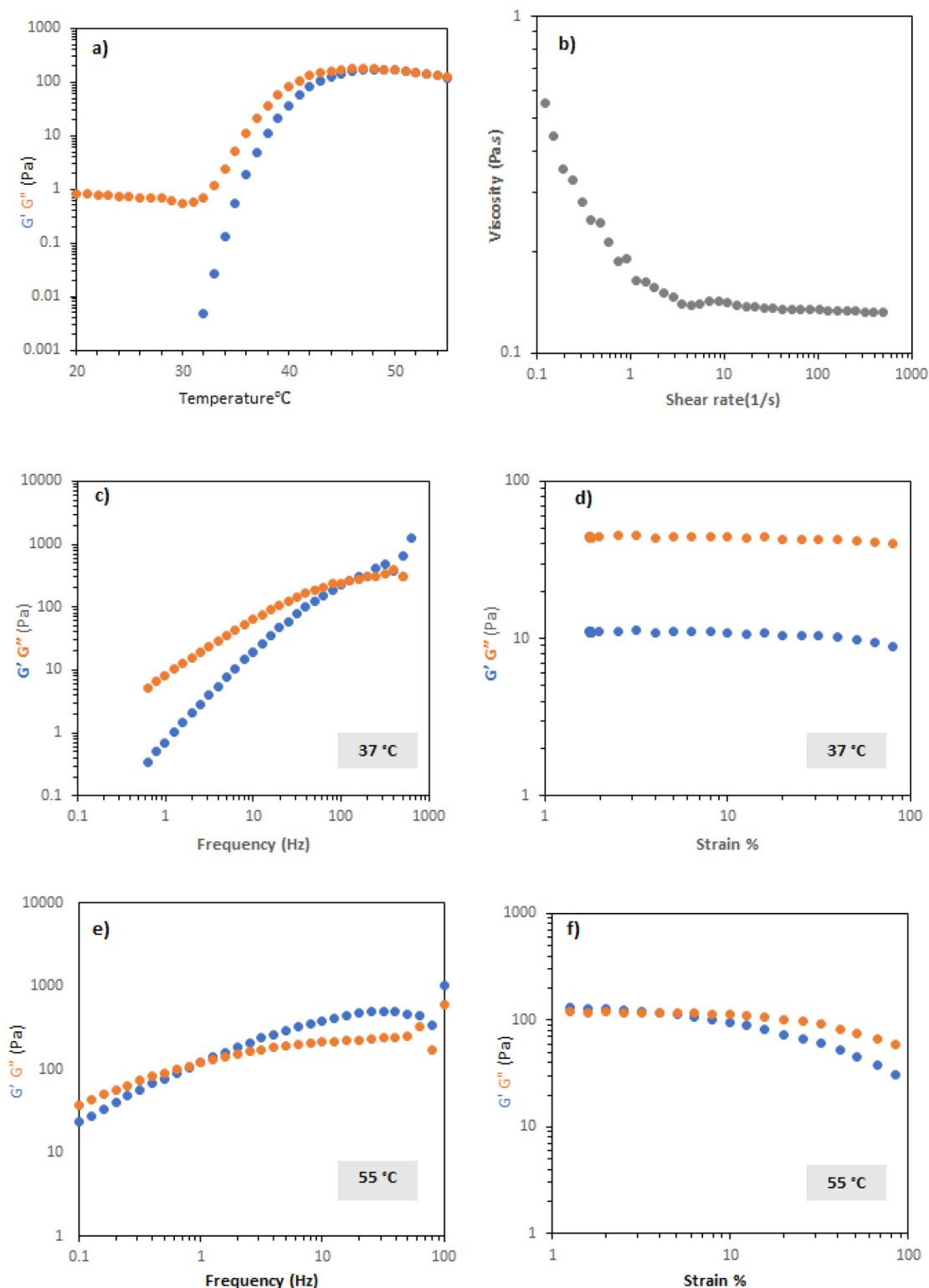


**Fig. 5** Rheological properties of PNIPAM-*b*-PEO-*b*-PNIPAM solution at concentration 20% (w/v): (a) temperature ramps at a fixed strain (0.1%) and frequency (6.283 rad per s). (b) Flow rheology at 20 °C. (c) Frequency sweeps at 0.1% strain and 37 °C. (d) Amplitude sweeps at 6.283 rad per s and 37 °C. (e) Frequency sweeps at 0.1% strain and 55 °C. (f) Amplitude sweeps at 6.283 rad per s and 55 °C.

modulated by physical and mechanical cues such as surface roughness and the polymers used as biomaterials.<sup>43,44</sup> Yet the majority of studies of alveolar macrophages activation and

responses to external stimuli have been performed in conventional 2D culture systems. As it has been reported in many studies that 2D models are unable to represent tissue cells



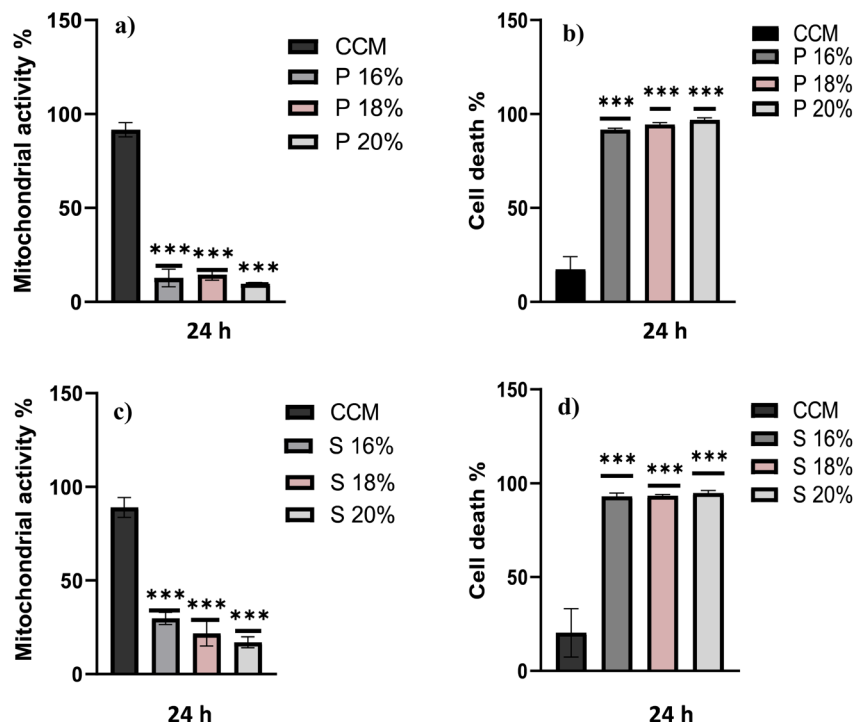


**Fig. 6** Assessment of Poloxamer 407 (P) and Soluplus (S) polymers on cell health of alveolar-like macrophages *in vitro*. ImmuPHAGE were incubated with filtered hydrogels for 24 h. Mitochondrial activity (a and c) was assessed using MTS assay, and data were presented as percentage of viable cells in comparison to cells cultured in CCM. Membrane integrity (b and d) was assessed with Trypan blue and presented as percentage of dead cells embedded in gels. Data are expressed as mean values of  $n = 4$  wells replicates  $\pm$  SD, and statistical significance is marked as follows: \*\*\*indicates  $p < 0.001$ .

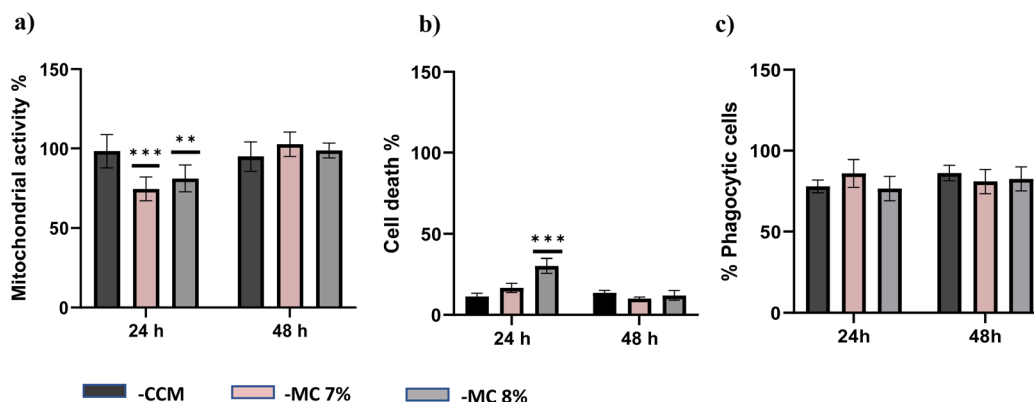


**Fig. 7** Assessment of ImmuPHAGE cells following incubation with MC 7% (MC 7%) and 8% (MC 8%). Mitochondrial activity (a) was assessed using MTS assay, and data were expressed as percentage of viable cells. Membrane integrity (b) using propidium iodide assay was expressed as a percentage of dead cells. Phagocytic activity (c) of ImmuPHAGE cells was assessed at two different time points (24 h and 48 h). Percentage of phagocytic cells (c) was expressed as mean  $\pm$  SD of  $n = 3$  of each time points, and statistical significance is marked as follows: \*\*indicates  $p < 0.01$  and \*\*\*indicates  $p < 0.001$ .

*in vitro* as cells grown in 2D culture have altered morphology, which may influence many cellular responses, whereas 3D models more accurately resemble the *in vivo* conditions.<sup>45–47</sup> So this study aimed to select the most suitable polymer for a 3D culture where hydrogels as highly porous matrices are seen as good candidates for culturing immune cells, allowing them

to migrate as they would *in vivo* and maintain more *in vivo*-like properties. Consequently, that may provide a system allowing a closer *in vivo*-like morphology and functionality, providing more predictive macrophage cell responses to toxic stimuli. While this study seeks to evaluate the suitability of thermoreversible gels for use in immunocompetent cell



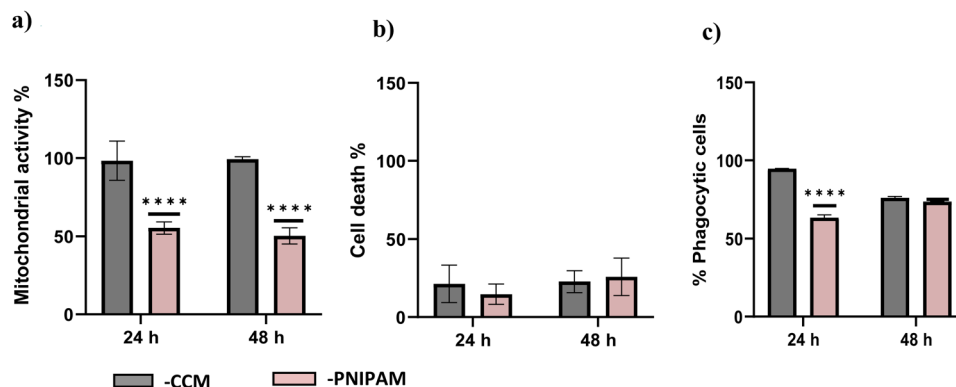


**Fig. 8** Assessment of ImmuPHAGE cells following incubation with PNIPAM. Cells were incubated with filtered hydrogels for 24 and 48 h. Mitochondrial activity (a) was assessed using MTS and Membrane integrity LDH (b), data were expressed as percentage of dead cells in comparison to CCM control. Percentage of phagocytic cells (c) was expressed as mean  $\pm$  SD of  $n = 3$  of each time points, and statistical significance is marked as follows: \*indicates  $p < 0.05$ , and \*\*\*indicates  $p < 0.001$ .

models containing ImmuPHAGE, the follow-up studies will evaluate the impact of selected polymers in cell phenotype, morphology and responses to various chemicals.

This study tested four different polymers: Poloxamer 407, Soluplus, MC and PNIPAM-*b*-PEO-*b*-PNIPAM. Initially, the physical properties of all polymers were visually tested to decide on suitable concentrations before their rheological properties were characterised. All polymers exhibited thermoreversible gel formation by vial inversion with  $T_{gel}$  in the target temperature range (25–37 °C) within concentrations determined by the pilot study. The rheological analysis allowed for additional information about the gel state, as well as flow properties of the room temperature solution, to probe the ability to manipulate the materials in this form. Soluplus, PNIPAM-*b*-PEO-*b*-PNIPAM and Poloxamer 407 typically exhibited a high degree of shear thinning to low viscosity at high shear. This aligns with the visual observation that the materials were easily extruded through a pipette. MC showed a low degree of shear thinning behaviour, and as such, there was difficulty in manipulating the material at room temperature. In addition to these rheological differences at room temperature, there was a diversity of behaviours in the “gel” state. MC and Poloxamer 407 exhibited a low dependence of  $G'$  and  $G''$  on frequency, with  $\tan \delta < 1$  at all frequencies. These materials are, therefore, not predicted to exhibit flow over the frequencies measured and are expected to retain their shape in the gel state. Soluplus and PNIPAM-*b*-PEO-*b*-PNIPAM exhibited Maxwell-type rheology at 37 °C, and there is the potential for flow to occur over long timescales. From an entirely rheological standpoint, Poloxamer 407 exhibited the most desirable profile, with a low viscosity shear thinning solution state at 20 °C but a permanent gel state at 37 °C, albeit brittle with a low yield strain.

The biological compatibility of these polymers was assessed using human cell cultures representative of alveolar macrophage-like cells, ImmuPHAGE. Three different concentrations of Poloxamer 407 and Soluplus were used to test their

biocompatibility after 24 h incubation. Both assays performed (MTS and trypan blue) showed a significant decrease ( $p < 0.05$ ) in cell viability of cells embedded in gels in comparison to cells cultured in CCM (Fig. 5). Therefore, it can be concluded that Poloxamer 407 and Soluplus do not support the growth of cells, and they are unsuitable scaffold materials for culturing these cells *in vitro*. This is likely to be attributed to the fact that both polymers exhibit surfactant-like properties due to their amphiphilic structure, which makes them ideal for use in the cosmetic industry and gives them a range of pharmaceutical applications, such as biomaterials for bio-printing.<sup>48</sup> However, surfactants as surface active materials interfere with cell membranes by reducing surface tension and disrupting the typical architecture of lipid bilayer, resulting in cell lysis.<sup>48</sup>

Even though many studies demonstrate that some cell lines remain viable in the presence of PNIPAM, it has been reported to be cytotoxic to smooth muscle cells and fibroblasts.<sup>49,50</sup> ImmuPHAGE encapsulated into this hydrogel dropped their metabolic activity whilst their membrane integrity and phagocytic activity remained (Fig. 7). According to Partearroyo *et al.* (1990), critical micellar concentration has a crucial role on cell-polymer interaction, they also demonstrated that loss of cell viability occurs at surfactant concentrations below the critical micellar concentration while cell lysis only occurs at or near the critical micellar concentration.<sup>51</sup> As stated above, the cytotoxicity of PNIPAM is dependent upon the cell type used. The biocompatibility of MC has previously been demonstrated with different cell lines.<sup>52–54</sup> Additionally, our findings showed that MC at concentrations 7% and 8% can support 3D growth of ImmuPHAGE over the time period tested (Fig. 6) without affecting cell viability. Hence, from all tested polymers, MC represents the most promising matrix that merits further evaluation, possibly optimising/mixing with other polymers could show mechanical and rheological synergism.<sup>55</sup> The time-point chosen in this preliminary study represents the most typical time points used in inhalation toxicity screening.<sup>55</sup>





## Conclusions

Thermoreversible gels offer switchable sol–gel behaviour on temperature change. MC, soluplus, poloxamer 407, and PNIPAM-*b*-PEO-*b*-PNIPAM were explored in cell culture media to determine rheological performance for inclusion in immunocompetent models. Whilst soluplus and poloxamer 407 gave desirable rheological behaviours, their cellular compatibility was poor. MC, followed by PNIPAM-*b*-PEO-*b*-PNIPAM, could better maintain macrophage viability and functionality. Overall, thermoresponsive polymers exhibited simple cell isolation and recovery process as they do not rely on complex procedures such as extraction buffer or enzymatic treatment for cell recovery from 3D cell cultures.<sup>56,57</sup> Additionally, polymers from defined composition are seen as potential biomaterials that could be used to establish new, reliable and cost-effective 3D cell culture models. These systems also have the potential to drive next-generation 3D models that more accurately represent humans and provide better cell function and response to *in vivo* situations.

## Conflicts of interest

Victoria Hutter and Ewelina Hoffman are employees of ImmuONE.

## Acknowledgements

Amjad Saeed is thanked for providing training and support to EZ. EPSRC are acknowledged for funding MC and MAS via a New Investigator award (EP/T00813X/1).

## References

- 1 A. O. Fels and Z. A. Cohn, The alveolar macrophage., *J. Appl. Physiol.*, 1986, **60**, 353–369.
- 2 R. M. Jones and N. Neef, Interpretation and prediction of inhaled drug particle accumulation in the lung and its associated toxicity, *Xenobiotica*, 2012, **42**, 86–93.
- 3 B. Forbes, R. O'Lone, P. P. Allen, A. Cahn, C. Clarke, M. Collinge, L. A. Dailey, L. E. Donnelly, J. Dybowski, D. Hassall, D. Hildebrand, R. Jones, J. Kilgour, J. Klapwijk, C. C. Maier, T. McGovern, K. Nikula, J. D. Parry, M. D. Reed, I. Robinson, L. Tomlinson and A. Wolfreys, Challenges for inhaled drug discovery and development: Induced alveolar macrophage responses, *Adv. Drug Delivery Rev.*, 2014, **71**, 15–33.
- 4 K. J. Nikula, J. E. McCartney, T. McGovern, G. K. Miller, M. Odin, M. V. Pino and M. D. Reed, STP position paper: interpreting the significance of increased alveolar macrophages in rodents following inhalation of pharmaceutical materials, *Toxicol. Pathol.*, 2014, **42**, 472–486.
- 5 D. S. Warren, S. P. H. Sutherland, J. Y. Kao, G. R. Weal and S. M. Mackay, The Preparation and Simple Analysis of a Clay Nanoparticle Composite Hydrogel, *J. Chem. Educ.*, 2017, **94**, 1772–1779.
- 6 E. Caló and V. V. Khutoryanskiy, Biomedical applications of hydrogels: a review of patents and commercial products, *Eur. Polym. J.*, 2014, **65**, 252–267.
- 7 M. Bahram, N. Mohseni and M. Moghtader, in *Emerging Concepts in Analysis and Applications of Hydrogels*, InTech, 2016.
- 8 M. Patel, H. J. Lee, S. Park, Y. Kim and B. Jeong, Injectable thermogel for 3D culture of stem cells, *Biomaterials*, 2018, **159**, 91–107.
- 9 L. E. Bromberg and E. S. Ron, Temperature-responsive gels and thermogelling polymer matrices for protein and peptide delivery, *Adv. Drug Delivery Rev.*, 1998, **31**, 197–221.
- 10 M. Karimi, A. Ghasemi, P. Sahandi Zangabad, R. Rahighi, S. Masoud Moosavi Basri, H. Mirshekari, M. Amiri, Z. Shafaei Pishabad, A. Aslani, M. Bozorgomid, D. Ghosh, A. Beyzavi, A. Vaseghi, A. R. Aref, L. Haghani, S. Bahrami and M. R. Hamblin, Smart micro/nanoparticles in stimulus-responsive drug/gene delivery systems, *Chem. Soc. Rev.*, 2016, **45**, 1457–1501.
- 11 L. Yu and J. Ding, Injectable hydrogels as unique biomedical materials, *Chem. Soc. Rev.*, 2008, **37**, 1473–1481.
- 12 J. D. Kretlow, L. Klouda and A. G. Mikos, Injectable matrices and scaffolds for drug delivery in tissue engineering, *Adv. Drug Delivery Rev.*, 2007, **59**, 263–273.
- 13 A. Chiappone, E. Fantino, I. Roppolo, M. Lorusso, D. Manfredi, P. Fino, C. F. Pirri and F. Calignano, 3D Printed PEG-Based Hybrid Nanocomposites Obtained by Sol–Gel Technique, *ACS Appl. Mater. Interfaces*, 2016, **8**, 5627–5633.
- 14 P. Haddow, W. J. McAuley, S. B. Kirton and M. T. Cook, Poly(N-isopropyl acrylamide)  $\bar{n}$  poly(ethylene glycol)  $\bar{n}$  poly(N-isopropyl acrylamide) as a thermoreversible gelator for topical administration, *Mater. Adv.*, 2020, **1**, 371–386.
- 15 A. M. Bodratti and P. Alexandridis, Formulation of Poloxamers for Drug Delivery, *J. Funct. Biomater.*, 2018, **9**(11), 1–24.
- 16 M. A. Abou-Shamat, J. Calvo-Castro, J. L. Stair and M. T. Cook, Modifying the Properties of Thermogelling Poloxamer 407 Solutions through Covalent Modification and the Use of Polymer Additives, *Macromol. Chem. Phys.*, 2019, **220**, 1900173.
- 17 P. Alexandridis and T. A. Hatton, Poly(ethylene oxide) poly(propylene oxide) poly(ethylene oxide) block copolymer surfactants in aqueous solutions and at interfaces: thermodynamics, structure, dynamics, and modeling, *Colloids Surf.*, A, 1995, **96**, 1–46.
- 18 J. Juhasz, V. Lenaerts, P. Raymond and H. Ong, Diffusion of rat atrial natriuretic factor in thermoreversible poloxamer gels., *Biomaterials*, 1989, **10**, 265–268.
- 19 I. Salah, M. A. Shamat and M. T. Cook, Soluplus solutions as thermothickening materials for topical drug delivery, *J. Appl. Polym. Sci.*, 2019, **136**, 46915.
- 20 H. H. Lin and Y. L. Cheng, *In situ* thermoreversible gelation of block and star copolymers of poly(ethylene glycol) and



- poly(*n*-isopropylacrylamide) of varying architectures, *Macromolecules*, 2001, **34**, 3710–3715.
- 21 C. Sofroniou, M. Baglioni, M. Mamusa, C. Resta, J. Douch, J. Smets and P. Baglioni, Self-Assembly of Soluplus in Aqueous Solutions: Characterization and Prospectives on Perfume Encapsulation, *ACS Appl. Mater. Interfaces*, 2022, **14**, 14791–14804.
  - 22 N. A. Cortez-Lemus and A. Licea-Claverie, *Prog. Polym. Sci.*, 2016, **53**, 1–51.
  - 23 M. T. Cook, P. Haddow, S. B. Kirton and W. J. McAuley, *Adv. Funct. Mater.*, 2021, **31**, 2008123.
  - 24 M. Cespi, L. Casettari, G. F. Palmieri, D. R. Perinelli and G. Bonacucina, Rheological characterization of polyvinyl caprolactam–polyvinyl acetate–polyethylene glycol graft copolymer (Soluplus®) water dispersions, *Colloid Polym. Sci.*, 2014, **292**, 235–241.
  - 25 N. Sarkar, Thermal gelation properties of methyl and hydroxypropyl methylcellulose, *J. Appl. Polym. Sci.*, 1979, **24**, 1073–1087.
  - 26 P. L. Nasatto, F. Pignon, J. L. M. Silveira, M. E. R. Duarte, M. D. Nosedá and M. Rinaudo, Methylcellulose, a cellulose derivative with original physical properties and extended applications, *Polymers*, 2015, **7**, 777–803.
  - 27 A. Haque and E. R. Morris, Thermogelation of methylcellulose. Part I: molecular structures and processes, *Carbohydr. Polym.*, 1993, **22**, 161–173.
  - 28 P. P. Kundu, M. Kundu, M. Sinha, S. Choe and D. Chattopadhyay, Effect of alcoholic, glycolic, and polyester resin additives on the gelation of dilute solution (1%) of methylcellulose, *Carbohydr. Polym.*, 2003, **51**, 57–61.
  - 29 N. Sarkar and L. C. Walker, Hydration–dehydration properties of methylcellulose and hydroxypropyl-methylcellulose, *Carbohydr. Polym.*, 1995, **27**, 177–185.
  - 30 S. Thirumala, J. Gimble and R. Devireddy, Methylcellulose Based Thermally Reversible Hydrogel System for Tissue Engineering Applications, *Cells*, 2013, **2**, 460–475.
  - 31 B. Jeong, S. W. Kim and Y. H. Bae, Thermosensitive sol-gel reversible hydrogels, *Adv. Drug Delivery Rev.*, 2012, **64**, 154–162.
  - 32 M. A. da Silva, P. Haddow, S. B. Kirton, W. J. McAuley, L. Porcar, C. A. Dreiss and M. T. Cook, Thermoresponsive Triblock-Copolymers of Polyethylene Oxide and Polymethacrylates: Linking Chemistry, Nanoscale Morphology, and Rheological Properties, *Adv. Funct. Mater.*, 2021, **32**, 2109010.
  - 33 F. Doberenz, K. Zeng, C. Willems, K. Zhang and T. Groth, Thermoresponsive polymers and their biomedical application in tissue engineering—A review, *J. Mater. Chem. B*, 2020, **8**, 607–628.
  - 34 E. Hodder, S. Duin, D. Kilian, T. Ahlfeld, J. Seidel, C. Nachtigall, P. Bush, D. Covill, M. Gelinsky and A. Lode, Investigating the effect of sterilisation methods on the physical properties and cytocompatibility of methyl cellulose used in combination with alginate for 3D-bioplotting of chondrocytes, *J. Mater. Sci.: Mater. Med.*, 2019, **30**, 1–16.
  - 35 A. L. Niles, R. A. Moravec and T. L. Riss, In vitro viability and cytotoxicity testing and same-well multi-parametric combinations for high throughput screening, *Curr. Chem. Genomics Transl. Med.*, 2009, **11**(3), 33–41.
  - 36 E. Hoffman, N. Perez-Diaz, A. Saeed, R. Mahendran, V. Hutter and A. Martin, Novel alveolar macrophage-like model (ImmuPHAGE) as a platform for better mechanistic understanding for the fate of inhaled medicines, *ERJ Open Res.*, 2022, **8**(8), 98.
  - 37 J. Desbrières, M. Hirrien and S. B. Ross-Murphy, Thermogelation of methylcellulose: rheological considerations, *Polymer*, 2000, **41**, 2451–2461.
  - 38 M. A. Da Silva, I. A. Farhat, E. P. G. Arêas and J. R. Mitchell, Solvent-induced lysozyme gels: Effects of system composition and temperature on structural and dynamic characteristics, *Biopolymers*, 2006, **83**, 443–454.
  - 39 S. R. Polio, A. N. Kundu, C. E. Dougan, N. P. Birch, D. Ezra Aurian-Blajeni, J. D. Schiffman, A. J. Crosby and S. R. Peyton, Cross-platform mechanical characterization of lung tissue, *PLoS One*, 2018, **13**(10), 1–17.
  - 40 E. A. Aisenbrey and W. L. Murphy, Synthetic alternatives to Matrigel, *Nat. Rev. Mater.*, 2020, **5**, 539–551.
  - 41 H. K. Kleinman and G. R. Martin, Matrigel: Basement membrane matrix with biological activity, *Semin. Cancer Biol.*, 2005, **15**, 378–386.
  - 42 J. Bystroňová, I. Ščigalková, L. Wolfová, M. Pravda, N. E. Vrana and V. Velebný, Creating a 3D microenvironment for monocyte cultivation: ECM-mimicking hydrogels based on gelatine and hyaluronic acid derivatives, *RSC Adv.*, 2018, **8**, 7606–7614.
  - 43 B. Wójciak-Stothard, Z. Madeja, W. Korohoda, A. Curtis and C. Wilkinson, Activation of macrophage-like cells by multiple grooved substrata. Topographical control of cell behaviour., *Cell Biol. Int.*, 1995, **19**, 485–490.
  - 44 F. Y. McWhorter, C. T. Davis and W. F. Liu, Physical and mechanical regulation of macrophage phenotype and function, *Cell. Mol. Life Sci.*, 2015, **72**, 1303–1316.
  - 45 O. Zschenker, T. Streichert, S. Hehlhans and N. Cordes, Genome-Wide Gene Expression Analysis in Cancer Cells Reveals 3D Growth to Affect ECM and Processes Associated with Cell Adhesion but Not DNA Repair, *PLoS One*, 2012, **7**(4), e34279.
  - 46 G. Mahmud, C. J. Campbell, K. J. M. Bishop, Y. A. Komarova, O. Chaga, S. Soh, S. Huda, K. Kandere-Grzybowska and B. A. Grzybowski, Directing cell motions on micropatterned ratchets, *Nat. Phys.*, 2009, **5**, 606–612.
  - 47 C. H. Thomas, J. H. Collier, C. S. Sfeir and K. E. Healy, Engineering gene expression and protein synthesis by modulation of nuclear shape, *Proc. Natl. Acad. Sci. U. S. A.*, 2002, **99**, 1972–1977.
  - 48 M. T. Cook, P. Haddow, S. B. Kirton and W. J. McAuley, Polymers Exhibiting Lower Critical Solution Temperatures as a Route to Thermoreversible Gelators for Healthcare, *Adv. Funct. Mater.*, 2021, **31**, 2008123.
  - 49 M. A. Cooperstein, P. A. H. Nguyen and H. E. Canavan, Poly (N-isopropyl acrylamide)-coated surfaces: Investigation of



- the mechanism of cell detachment, *Biointerphases*, 2017, **12**(12), 02C401-1.
- 50 H. Vihola, A. Laukkanen, L. Valtola, H. Tenhu and J. Hirvonen, Cytotoxicity of thermosensitive polymers poly (N-isopropylacrylamide), poly(N-vinylcaprolactam) and amphiphilically modified poly(N-vinylcaprolactam), *Biomaterials*, 2005, **26**, 3055–3064.
  - 51 M. A. Partearroyo, H. Ostolaza, F. M. Goñi and E. Barberá-Guillem, Surfactant-induced cell toxicity and cell lysis: A study using B16 melanoma cells, *Biochem. Pharmacol.*, 1990, **40**, 1323–1328.
  - 52 M. J. Caicco, T. Zahir, A. J. Mothe, B. G. Ballios, A. J. Kihm, C. H. Tator and M. S. Shoichet, Characterization of hyaluronan–methylcellulose hydrogels for cell delivery to the injured spinal cord, *J. Biomed. Mater. Res., Part A*, 2013, **101**, 1472–1477.
  - 53 C.-H. Chen, C.-C. Tsai, W. Chen, F.-L. Mi, H.-F. Liang, S.-C. Chen and H.-W. Sung, Novel living cell sheet harvest system composed of thermoreversible methylcellulose hydrogels, *Biomacromolecules*, 2006, **7**, 736–743.
  - 54 A. Mahboubian, D. Vllasaliu, F. A. Dorkoosh and S. Stolnik, Temperature-Responsive Methylcellulose–Hyaluronic Hydrogel as a 3D Cell Culture Matrix, *Biomacromolecules*, 2020, **21**, 4737–4746.
  - 55 T. Hoare, D. Zurakowski, R. Langer and D. S. Kohane, Rheological blends for drug delivery. I. Characterization in vitro, *J. Biomed. Mater. Res., Part A*, 2010, **92**(2), 575–585.
  - 56 A. S. Johnson, E. O'Sullivan, L. N. D'Aoust, A. Omer, S. Bonner-Weir, R. J. Fisher, G. C. Weir and C. K. Colton, Quantitative assessment of islets of Langerhans encapsulated in alginate, *Tissue Eng., Part C*, 2011, **17**, 435–449.
  - 57 Z. Li, M. Leung, R. Hopper, R. Ellenbogen and M. Zhang, Feeder-free self-renewal of human embryonic stem cells in 3D porous natural polymer scaffolds, *Biomaterials*, 2010, **31**, 404–412.

